ABDOMINAL CHARACTERIZATION UNDER LAP BELT LOADING

Taewung Kim
Gwansik Park
Salvador Montesinos
Damien Subit
James Bolton
Brian Overby
Jason Forman
Jeff Crandall
University of Virginia Center for Applied Biomechanics
USA

Hyungjoo Kim
Hyundai Motor Group
South Korea

Paper Number 15-0312

ABSTRACT

The phenomenon of submarining is of major interest in the design and optimization of restraint systems. A biofidelic finite element human body model can be more useful for investigating this phenomenon than the existing dummy. For the validation of finite element human body models, belt pull tests were performed to characterize thoracic and abdominal regions of the PMHS, and the 50%tile male Hybrid III dummy was tested for comparison with the PMHS. The spines of subjects were rigidly mounted to a test fixture through a mounting system to minimize the influence of the spinal motion during the test. The pelvis of the subjects were positioned close to the normal driving posture, but the torso angle was more reclined than the average driving posture due to the difficulty of adjusting the torso angle during the mounting process. This torso angle led to the belt being positioned more rearward with respect to anterior superior iliac spine (ASIS) in the longitudinal direction. The subjects were loaded under lap belt only configurations with two levels of load limits, 1 kN and 3 kN. The lap belt was positioned in various vertical offsets with respect to ASIS and belt angles. The vertical offset of the belt from ASIS was determined based on volunteer test data. Belt pulling distance, belt cable force, spine reaction force, and belt kinematics were documented for the human body model validation. During the lap belt tests, both belt sliding over the pelvis and belt staying in front of the pelvis were observed, and a large amount of abdominal compression was observed during the submarining cases. After finishing the test series, autopsies were performed on the PMHS, and both PMHS showed no injuries in the abdominal region. One of the PMHS also showed a pelvic fracture at the iliac crest, but the PMHS had a pre-existing healed pelvic fracture at the same location. It was believed that this pre-existing fracture had not healed completely prior to death. Note that its ASIS region was intact so it should not have affected the occurrence of the submarining-like belt kinematics. Although only two PMHS were tested, the biomechanical responses collected through the belt pull test can be used to validate the computational human body model for further investigation on the submarining phenomenon.

INTRODUCTION

Submarining is one of the major concerns in restraint system design. Lamielle et al. (2006) showed grown relative importance of abdominal injury due to the greater reduction in severe or fatal injuries in head and thorax than in the abdominal region. Poplin et al. (2014) showed that increased speed and the resulting crash delta V increases risk of AIS 2+ injuries to the hollow organs of the abdomen and suggested that direct loading from lap belts into lower abdomen seems to be one of the mechanisms of the abdominal injuries. Adomeit and Hegar (1975) pointed out that the occurrence of submarining harmfult to an occupant during a vehicular crash not only because the belt directly loads the abdominal region but also it can increase the risk of the thoracic injury and the lower extremity injury due to greater pelvic motion and loading the lower torso by shoulder belt due to reclined posture of an occupant, respectivley.

Abdominal characterization tests have been performed focusing on the abdominal region but initial lap belt to pelvis interaction or the driving posture of PMHS were not given much consideration during those tests (Foster et al., 2006, Lamielle et al., 2008). The subjects were positioned the belt at mid-umbilicus and pulled horizontally by only engaging the abdominal region. While the biomechanical test data collected from these two studies provide rich information to validate the abdominal region, it does not provide information on the initial interaction between the belt and the pelvis.

Uriot et al. (2006) studied the interaction between the lap belt and the pelvic region using a component level belt pull test by rotating the pulling direction. This study characterized the behavior of the pelvic region under lap belt loading conditions, but the belt was initially positioned below the ASIS. Note that Reed et al. (2013) found that out-of-position belt fit, which means wearing the lap belt over the ASIS, was prevalent from their volunteer belt fit study. This suggests the importance of characterizing the lap belt to abdominal and pelvic region interation under out-of-position belt fit.

The finite element human body model has the potential to investigate the submarinig phenominon since the current anthropomorphic test devices showed substantial difference in behavior while interacting with a lap belt under submarining at risk conditions (Uriot et al., 2006, Luet et al., 2012).

In the current study, an abdomonial characterization test using a lap belt was performed with for the average pelvic angle of driving posture. The belt was positioned around and above the ASIS based on the volunteer belt fit study (Reed et al., 2013) The spine was fixed to isolate the chracteristics of the abdominal region from other body regions. Belt force, belt displacement, and belt kinematics in 3-dimensional space were documented to aid computational model validation.

METHOD

Specimen and Specimen Preparation

Two female PMHS with similar statures but different weights, a health weight and an obese, were subjected to lap belt loading (Table 1). It was hyphothesized that females has higher risk of submarining due to their lower pelvis height compared to males. In addition to the PMHS, the 50th percentile male Hybrid III dummy was tested for comparison.

Table 1.
PMHS information

PMHS No.	683	700
Age	83	67
Gender	Female	Female
Height (cm)	168	165
Weight (kg)	68.0	84.4
Body Mass Index (BMI)	24.1 (Normal range)	31.0 (obese)
Spine mount location	Upper spine mount: C6, T2, T6, T8, T10, and T11-12 Lower spine mount: L2, L4, and sacrum	Upper: T1, T4, T7, T9, T11, and L1 Lower spine mount: L3, L5, sacrum

All PMHS specimens were screened for Hepatitis A, B, C, and HIV, as well as for pre-existing pathologies with the potential to influence thoracic properties. Pre-test radiographs and CT scans were taken to verify that specimens with acute or healed rib fractures or other pre-existing thoracic trauma were excluded from this study. All test procedures were approved by the University of Virginia cadaver institutional review board.

Test Rig

The test rig consisted of seat and seat back to support a subject, which was mounted onto the upper and lower spine mounts, and belt pull system (Figure 1 and Table 2). The design objectives for the test rig were to consider the shape of the abdominal skin of a typical driving situation during the interaction between the lap belt and the skin and to isolate the characteristics of the abdomen and pelvis from spinal motion for model validation purposes. The test fixture had 3 degrees of freedom to accommodate various sizes of subjects and to control belt angles. To prevent a parallel path for the vertical component of the belt force, the seat plate was positioned forward so that it did not support the pelvis. Since the hip joints of the PMHS were compliant in flexion and extension of the thigh, the seat load cell did not experience a substantial amount of vertical force.

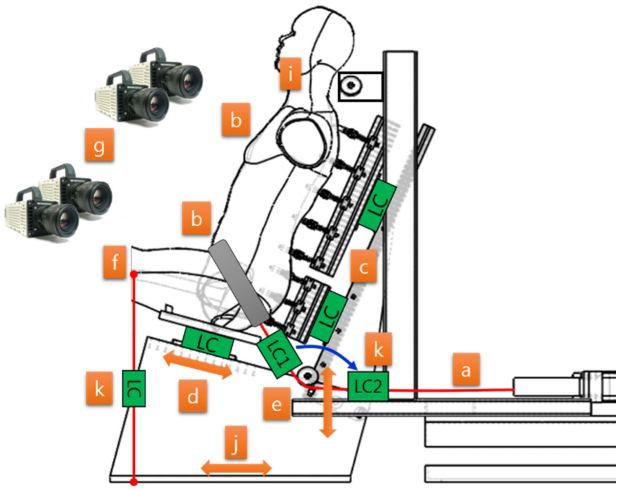

Figure 1. Schematic of belt pull test rig

Table 2.
Description of a belt pull test set-up

Item	Description
a	The belt cables attached to the belt ends were pulled by a pneumatic cylinder. A honeycomb was used to prevent excessive force applied to the PMHS.
b	A custom rigidized belt was placed on the abdomen and connected to the steel belt cables (see Custom rigidized belt).
c	Almost every other vertebra were mounted onto the upper and lower spine mounts. Six-axis loadcells (Model 2554AJ) were installed between the upper and lower spine mounts and the seat base. (see Spine mount)
d	A five-axis load cell was mounted under the seat to measure the reaction forces and moments.
e	The height of the anchor was adjusted to control the angle of the belt. The belt cable goes through a pulley to transmit the tensile force from the pneumatic cylinder to the belt. The distance between the left and right pulley was 560 mm.
f	The femurs were amputated and constrained to the seat bottom to prevent any upward motion of them.
g	Two Aramis optical displacement and strain mapping systems were used to track the 3-dimensional motion of the belt and deformation of the skin.
h	A uniaxial loadcell was placed in the cable that connected the femur and the seat base to measure tensile force in the cable.
i	Neck support was used to support the head due to the inactivity of the neck muscle.
j	The distance between the seat and seat back was adjustable to accommodate different sizes of subjects.
k	Belt cable loadcells were installed in the steel belt cable. It was moved from LC1 location fo LC2 location for the PMHS700 and the dummy tests.

Both ends of the belt was pulled by a pneumatic cylinder at the same speed (Figure 2), and the belt pulling force was measured using uniaxial belt cable loadcells on each end of the belt. Note that the belt cable loadcells were placed right next to the belt ends (LC1 in Figure 1) to exclude inertial and frictional force from pulleys for PMHS683 but it was moved to after the first pulley (LC2 in Figure 1) to resolve an initial slack problem in the belt. The belt pulling force was limited using a force limiting device by placing honeycomb between piston disk and belt pulling disk (Figure 2).

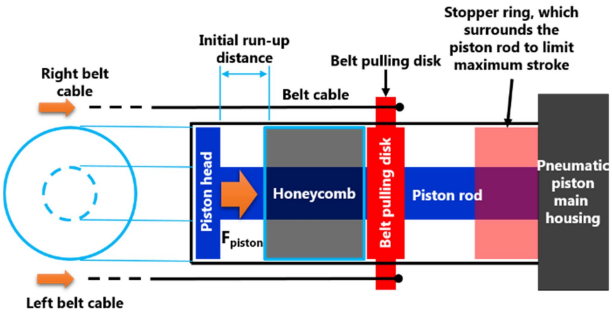

Figure 2. Load limiting device (top view)

<u>Spine mount</u> The spine mounts (Salzar et al., 2013), which were used for table-top tests, were installed to fix alternating vertebrae to the seat back (Figure 3). The thoracic spines were mounted to the upper spine mount column and the lumbar spine and sacrum, except L1 of PMHS700, were mounted to the lower spine mount column (Figure 1 and Table 2). Each spine mount had two degrees of freedom to adjust the pelvic angle and spine posture of the subject.

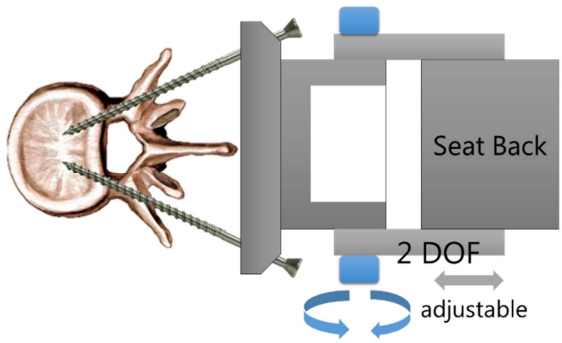

Figure 3. Spine mount (top view)

<u>Custom rigidized belt</u> The belt used in the current study was made of a polyethylene fiber-reinforced composite (Spectra®, E = 97 GPa) to minimize belt elongation (Salzar et al., 2013). The belt ends were clamped using metal plates and bolts (Figure 4), and steel belt cables were attached to each belt end to trasmit the pulling force from the pneumatic piston. The mass of the belt was tabulated to allow computational modeling of the belt since the inertial effect of the belt during the testing was not compensated in the belt pulling force in the Results section. There was belt slack during the PMHS683 tests due to the weights of the clamps and belt cable loadcell. To resolve this issue, another custom belt was built to lighten the weight, and the belt cable loadcell was moved from right next to the clamps to after the first pulley the belt cable went through.

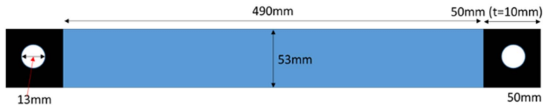

(a) Belt used for PMHS683

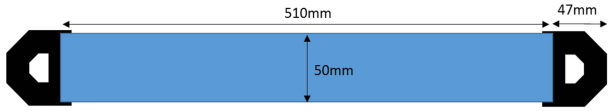

(b) Belt used for PMHS700 and Dummy
Figure 4. Belt geometry

Table 3.
Mass of belt and belt loadcell

Part	**Mass [g]**	
	PMHS683	PMHS700 and Dummy
belt	55	38
clamps	335	33
bolts on clamps	48	6
pins for the hole at belt ends	13	13
belt total (exc. loadcell)	451	90
belt loadcells	83	83

Instrumentation

<u>Sensor data</u> The force and moments from loadcells were filtered using CFC180 filter, and the belt displacement and belt 3-dimensional kinematics data was not filtered (Table 4). The belt pulling forces and displacements were not scaled for PMHS responses. Instead, the flesh thickness around the pelvic region was provided (see Flesh Thickness).

Table 4.
List of measurement for belt pull test

Measurement	Description	Filter
Belt force	belt cable loadcell (not inertially compensated for the mass of the belt, belt cable, and belt cable loadcells)	CFC180
Belt displacement	laser displacement sensor and video analysis	None
Reaction force and moment	6-axis spine mount loadcell	CFC180

Belt kinematics and skin deformation The Aramis optical displacement and strain mapping system (Aramis v6.2, GOM) was used to determine detailed kinematics of the belt, thorax, and abdomen of the subject during test. Note that the belt kinematics in the Results section was measured at the midline of the belt on the sagittal plane at the ASIS while the initial belt position in the Test matrix section was measured at the upper edge of the belt to follow Reed et al.'s method (2013). Lastly, a high speed x-ray system was used to record relative motion between belt and pelvis in sagittal plane during the lap belt test.

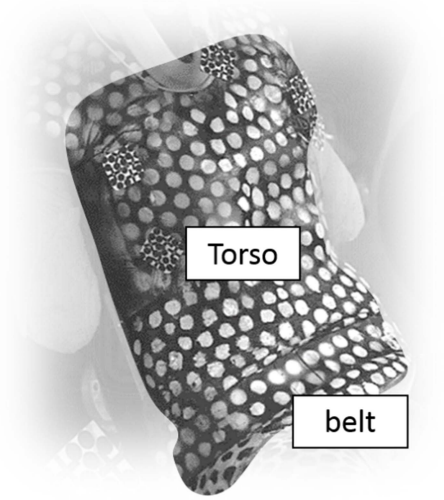

Figure 5 Pattern on the skin and belt for tracking

Test Condition

Coordinate Systems The SAE coordinate system was used to process the test data, and the upper right front corner of the seat was chosen as the origin for the global coordinate system (Figure 6). To obtain the desired belt position and angle, the seat was moved in X-direction and the D-ring and anchors were moved in Z-direction. Note that the positions of the D-ring and the anchors can be adjusted separately. Although the seat was moved during the positioning, the origin was attached to the front right corner of the top surface of the seat during data processing. In this way, only the positions of the anchors and the D-ring needed to be adjusted for the modeling.

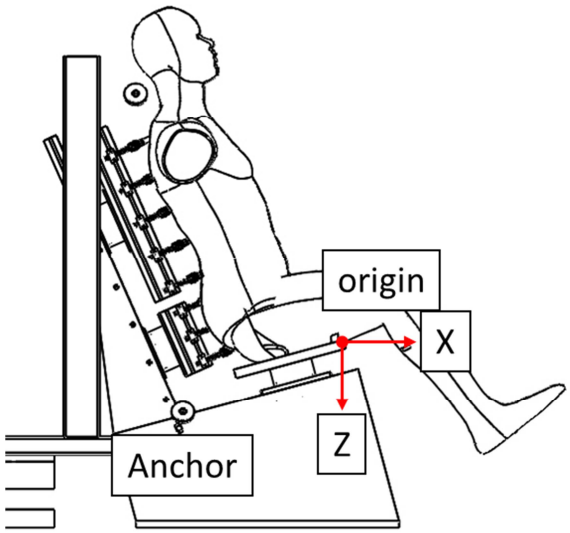

Figure 6 Global coordinate system and d-ring and anchor locations (origin: right front corner of the top surface of the seat)

PMHS and dummy positioning It was targetted to obtain 44 degrees of pelvic angle from vertical axis and C7 re ASIS X, which is a function of stature and BMI, was targeted to be around 265 mm. It was difficult to obtain the desired ASIS to C7 distance due to the range of adjustability of the spine mount system.

Table 5.
PMHS and dummy position

Measurement		PMHS683	PMHS700	Dummy
Pelvic angle [deg]	aft of vertical	44	37	55
	roll angle	-3	-5	0
ASIS to C7 (fore-aft) [mm]		304	347	285 (Upper and rearmost upper spine)

Definition of lap belt position The belt location was measured following the method used by Reed et al. (2013). The location of the upper edge of the belt was calculated by taking an average of the location of the upper edge at left and right sides of ASIS (anterior superior iliac spine) in the sagittal plane (Figure 7). Note that while Belt Z was within a range of Reed et al.'s volunteer belt fit tests during the belt pull test, Belt X was located more rearward due to the more reclined torso angle during the spine mounting.

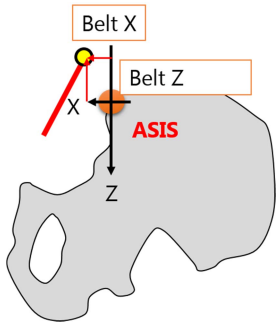

Figure 7 Belt position measurement

Test matrix Both the PMHS and the Hybrid III dummy were tested using a lap belt only condition by pulling both ends at the same time (Table 6). Although the belt was positioned to a target position based on the location of

ASIS from palpating on the skin during the tests, the calculated belt position, which was obtained by combining CT scan data of pelvis and spine mounts and belt position data from Aramis, were provided in Table 6. The lap belt angle was measured in the sagittal plane (XZ plane) using an inclinometer. Belt position, belt angle, belt force, and initial stroke rate were varied to see the effects of those on the responses of the abdominal area of the PMHS and the dummy. Note that the angles of belt and belt cable were different during PMHS683 tests due to relatively heavy weight of the belt clamps (Table 3) and the position of the belt cable loadcells.

Table 6
Test Matrix for PMHS683 (angle: X to -Z)

Test Name	Belt Upper Edge Position w.r.t ASIS (X, Z), Belt and Belt Cable Angles	Load limit (initial loading rate)	run#
PMHS683	(-8, -25) mm, belt cable: 52 deg, belt: 61 deg	1 kN (0 m/s)	3
	(-17, -31) mm, belt cable: 35 deg, belt: 55 deg	1 kN (0 m/s)	5
	(-16, -26) mm, belt cable: 44 deg, belt: 59 deg	3 kN (2 m/s)	7
PMHS700	(-12, -53) mm, 45 deg	1 kN (3 m/s)	3
	(-16, -55) mm, 45 deg	3 kN (4 m/s)	4
	(-46, -66) mm, 45 deg	1 kN (3 m/s)	5
	(-35, -69) mm, 45 deg	3 kN (4 m/s)	6
HybridIII	(22, -9) mm, 65 deg	3 kN (4 m/s)	6
	(22, -7) mm, 65 deg	1 kN (3 m/s)	7
	(15, -25) mm, 32 deg	1 kN (3 m/s)	8
	(7, -43) mm, 35 deg	1 kN (3 m/s)	9
	(7, -43) mm, 35 deg	3 kN (4 m/s)	10

RESULTS

Flesh Thickness

The flesh thickness of the the two PMHS and the dummy was measured on the sagittal plane at ASIS and mid-sagittal plane (Figure 8). The flesh thickness of PMHS683 was 15 mm and 38 mm on the sagittal plane at ASIS and the mid-point of ASIS of the subject, respectively. The flesh thickness of PMHS700 was 40 mm and 70 mm on the sagittal plane at ASIS and the mid-point of ASIS of the subject, respectively. The flesh thickness of the dummy was 25 mm and 63 mm on the sagittal planes at ASIS and at the mid-point of ASIS, respectively. Note that the geometry of the pelvis of the Hybrid III dummy is different from that of the PMHS. It does not have a protruded area at the tip of iliac wings like the PMHS.

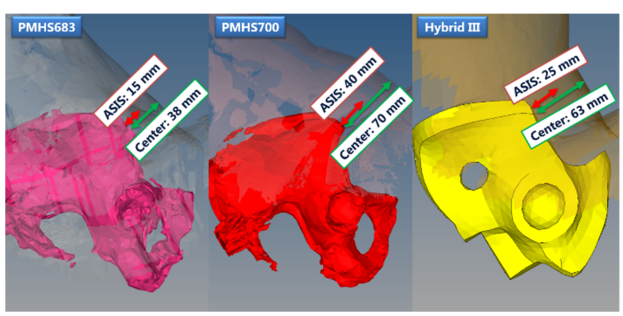

Figure 8 Flesh thickness around ASIS

Belt Kinematics and Belt Force

PMHS700 The time histories of belt pulling force and displacement and kinematics of the belt midline at ASIS were shown in Figure 9. The belt moved toward the pelvis at the beginning due to the initial belt angle and moved mostly horizontally afterwards. Although a honeycomb was used to limit the belt force, the belt pulling force exceeded the load limit in the beginning of the events as the belt loaded the pelvis through the flesh. Note that all

the honeycombs that were used in the testing were pre-crushed to ensure its limiting load. In the PMHS700-3 test, the belt slid over the iliac crest on the left side but caught near the ASIS on the right side. As the load limit increased and/or initial belt position heightened (Figure 9b-d), the belt completely slid over the pelvis in the end. Interestingly, once the belt completely slid over the iliac crest, the belt intrusion amounts into the abdomen were similar between low and high load limit cases (Figure 9c-d). The belt pulling force subsided after the belt slid over the iliac crest, and the belt stopped due to the limit of the range of motion of the pneumatic cylinder. The lower spine reaction force, which was the resultant force of F_x and F_z, showed similar peak forces for the lower load limit cases and lower peak forces for the higher load limit cases with time delays compared to the belt pulling forces.

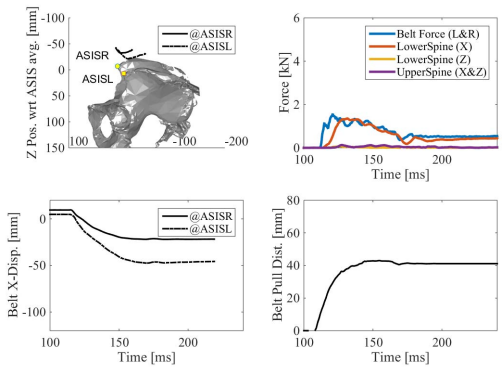

(a) PMHS700-3 (load limit, 1kN)

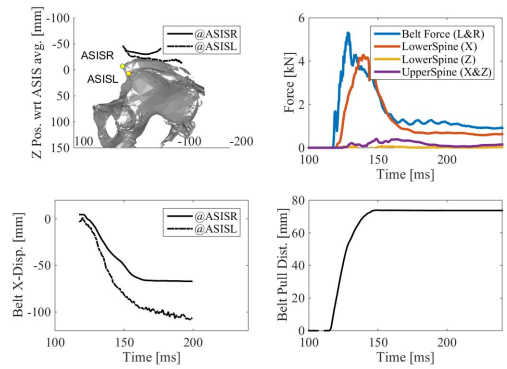

(b) PMHS700-4 (load limit, 3kN)

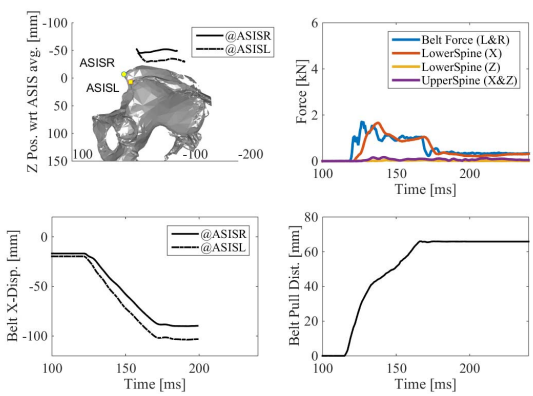

(c) PMHS700-5 (load limit, 1kN)

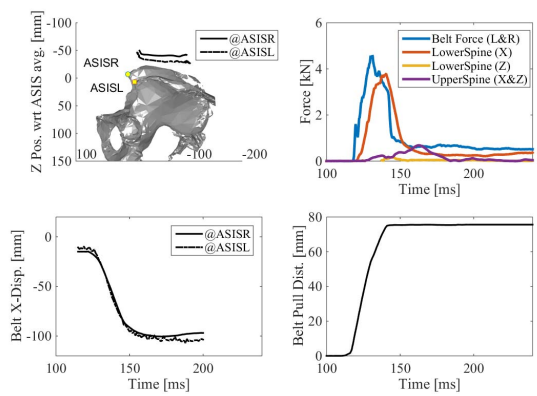

(d) PMHS700-6 (load limit, 3kN)

Figure 9. Belt pulling displacement and force time histories (PMHS700)

<u>PMHS683</u> Although the slack of the belt made the responses of the PMHS683 less desirable to use for model validation, the PMHS683 test provided belt kinematics both sliding over the pelvis (Figure 10a-b) and staying at the ASIS (Figure 10c). The belt showed downward motion when the belt stayed in front of the ASIS, and the maximum belt pulling distance was similar for the lower load limit (Figure 10a) and the higher load limit cases (Figure 10b). During the PMHS683-5 test, the belt moved toward the pelvis initially and slid over the pelvis in the end showing large amount of belt intrusion toward the abdomen (Figure 10c). The belt pulling force subsided to almost zero after the pneumatic piston reached its limit of range of motion. The belt was completely over the ASIS during the PMHS683-1 test (Figure 10d). The belt initially penetrated the abdomen due to 10 N of preload. With 1 kN of load limit, the belt intruded toward the abdomen more than 50 mm.

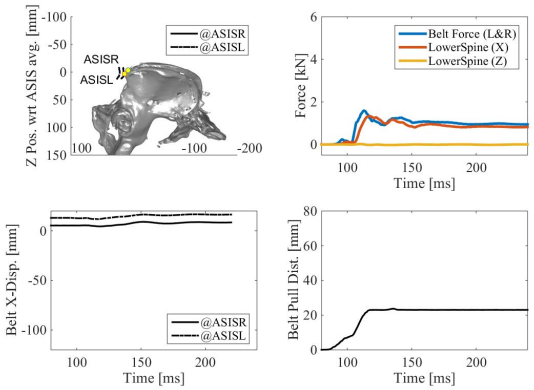

(a) PMHS683-3 (load limit, 1kN)

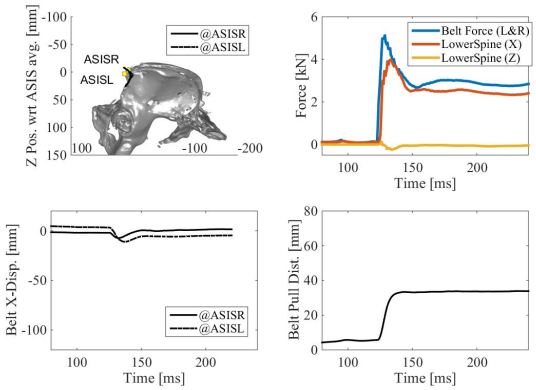

(b) PMHS683-7 (load limit, 3kN)

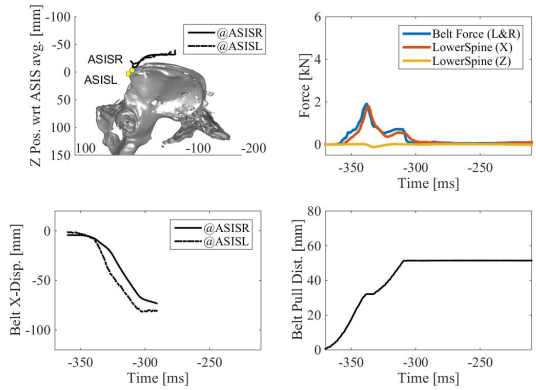

(c)PMHS683-5 (load limit, 1kN)

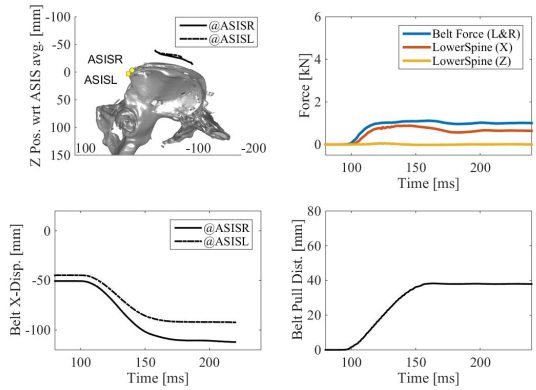

(d) PMHS683-1 (load limit, 1kN)

Figure 10. Belt pulling displacement and force time histories (PMHS683)

<u>High speed X-ray</u> The high speed x-ray was used during the PMHS683 tests (Figure 11). The x-ray images confirmed that the belt stayed in front of the pelvis during the PMHS683-3 and PMHS683-7 tests and it slid over the pelvis during PMHS683-5 tests. It was difficult to see the ASIS due to the over exposure around ASIS from the high speed x-ray images.

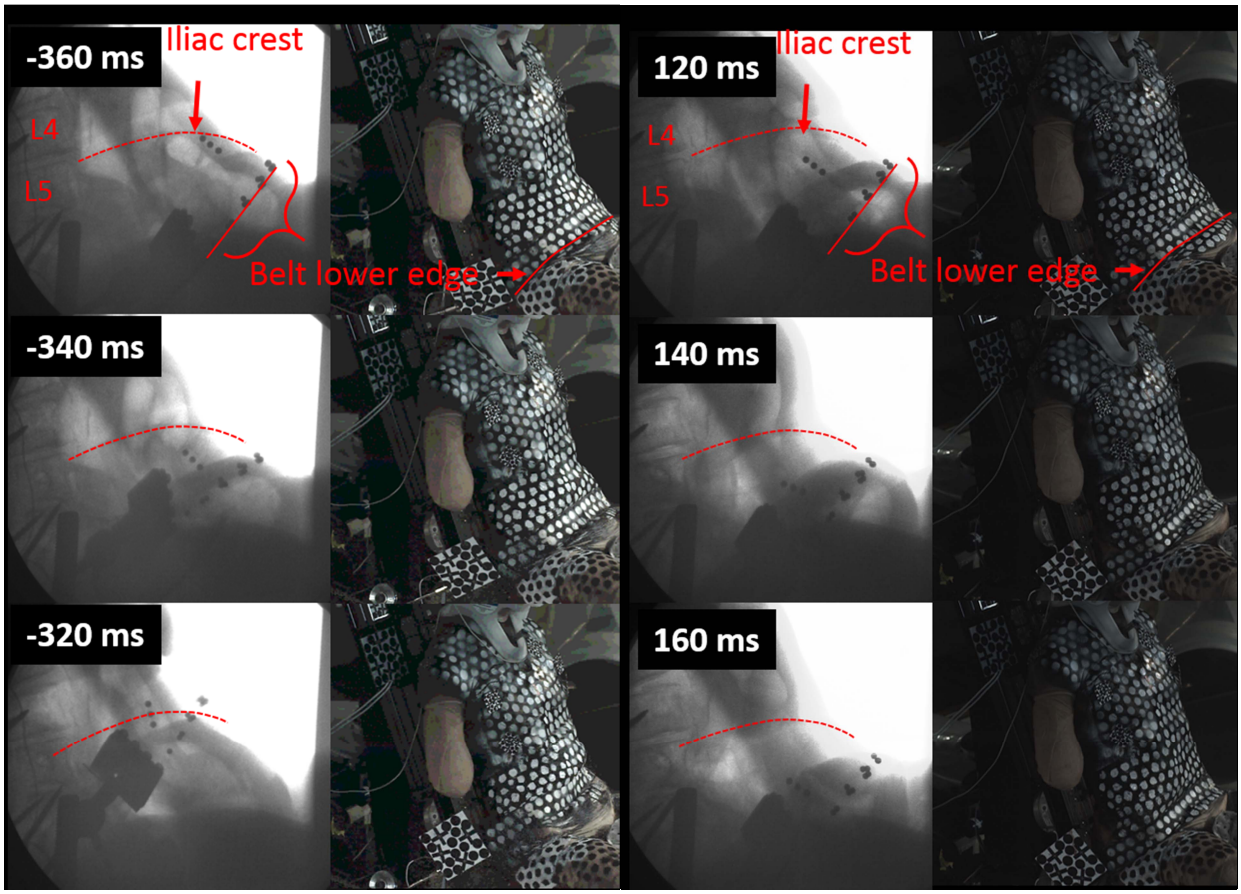

(a) PMHS683-5 *(b) PMHS683-7*

Figure 11 Snapshot of high speed x-ray

Hybrid III The belt did not completely slide over the pelvis during either HybridIII-9 (Figure 12a) or HybridIII-10 (Figure 12b) tests but the belt did show slight upward motion during the HybridIII-10 test. The dummy showed less belt intrusion (Figure 12b) toward the abdomen compared to both PMHS700-4 (Figure 9b) and PMHS683-5 (Figure 10c). Note that PMHS683-5 was tested with the 1kN of load limit while HybridIII-10 was tested with the 3 kN of load limit. The HybridIII-8 test (Figure 12c) showed lower peak belt pulling displacement than that of PMHS683-3 but this difference may come from the initial belt slack during the PMHS683-3 test. The HybridIII-6 test (Figure 12d) showed similar peak belt pulling displacement as that of PMHS683-7 (Figure 10b).

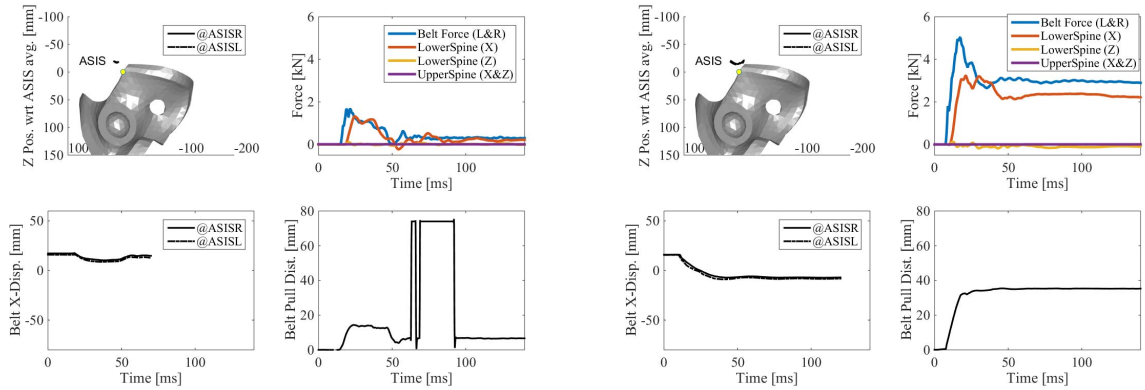

(a) HybridIII-9 (load limit, 1kN) (b) HybridIII-10 (load limit, 3kN)

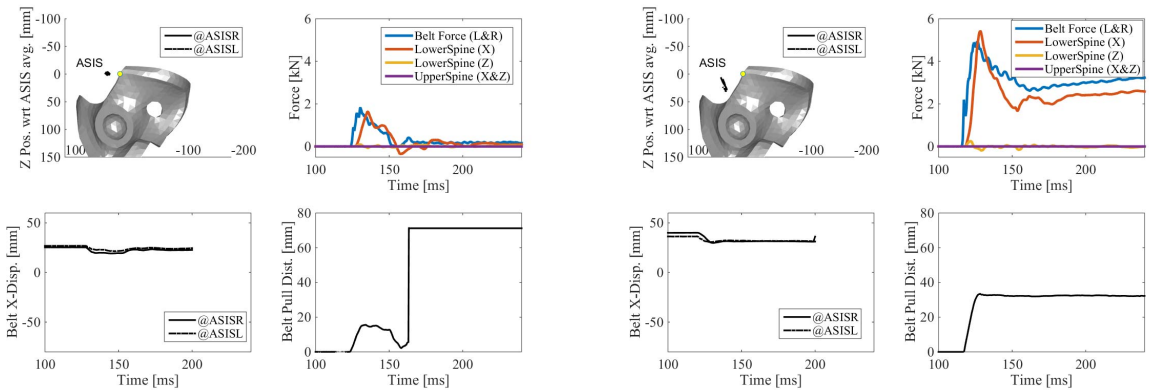

(a) HybridIII-8 (load limit, 1kN) (b) HybridIII-6 (load limit, 3kN)
Figure 12. Belt pulling displacement and force time histories (Hybrid III)

Injury Summary
Neither PMHS showed any signs of abdominal injury. PMHS683 showed a right iliac wing fracture and initially had a healed right iliac wing fracture. It seems that the right iliac wing of PMHS683 was not completely healed prior to death.

DISCUSSION

A new test rig to investigate subject to lap belt interaction was developed in the current study. To measure the belt kinematics, 3-dimensional motion tracking was used and provided useful information for understanding belt kinematics when the belt slid over the pelvis and for future computational model validation. Through the testing, the weight of the custom belt was reduced and the location of the belt cable loadcell was changed to resolve the belt initial slack issue. There was no initial slack issue with the older design of the custom belt on the table-top configuration, which was tested on subjects in a supine posture, but there was a problem in a seated posture.

An obese (PMHS700) and a normal weight (PMHS683) PMHS were tested in a seated posture under lap belt loading conditions to chracterize abdominal region. The belt was positioned near the ASIS and either slid over the pelvis or stayed in front of ASIS. With the aid of 3-dimensional motion tracking, the belt kinematics was well documented for validation of a computational human body model. Due to the belt slack issue in the PMHS683 tests, it was decided to use PMHS700 test results for human body model validation. Although there was a belt slack problem during the PMHS683 tests, the high speed x-ray images taken during the test confirmed that the belt kinematics measured using the Aramis system was reasonable.

For the cases that the belt slid over the pelvis, the belt force peaked in the beginning of the events while the belt was compressing the pelvis, and subsided while the belt slid over the pelvis. The reaction force from the spine mount

loadcells showed time delay, which indicates the inertial forces from the soft tissue and/or pelvis (Figure 10 and Figure 12). The PMHS700 showed larger time delays in lower spine reaction forces compared to the belt pulling forces than those of the PMHS683, and it may have stemmed from the heavier soft tissue of the PMHS700 (obese) than that of the PMHS683 (normal weight) (Table 1). It should be noted that the spine mounts that were holding the lumbar spine and pelvis showed the downward motion about 10 mm during the PMHS700-4 test (Figure 9b) from 132 ms to 145 ms, but it was after the lower spine reaction force reached 3.5 kN.

For the cases that the belt stayed on the pelvis, the belt showed little motion in X direction while showing about 20 mm of downward motion for 1 kN of load limit (Figure 10a and 30 mm of downward motion for 3 kN of load limit (Figure 10b). Although the high speed x-ray images provided qualitative information about the belt kinematics, it showed that the belt was at almost the same locations with respect to ASIS to that of the initial location at the end of the event. Therefore, the downward motion observed from the Aramis system was due to the pelvic rotation in Y direction rather than the belt sliding downward relative to ASIS (Figure 10a and b).

PMHS683-5 had 9 mm more rearward and 6 mm higher initial belt position than that of PMHS683-3 (Table 6). The 11 mm of difference in initial belt position drastically changed the test outcome (Figure 10a and c).

For model validaiton, the belt displacement time histories can be used as an input condition, and belt pulling force, spine reaction force, and the kinematics of the midline of the belt can be used as an target response. It will be important for a computation model to show the sudden increase of the belt pulling force in the beginning and the decrease of the belt pulling force afterwards with similar belt intrusion toward the abdomen prior to investigation of the submarining phenomenon. In addition, the model should be able to capture the transition between the belt sliding over the pelvis and the belt staying in front of the pelvis, for use in submarining investigation.

Althougth the current study limited due to small number of the PMHS and issues in the test fixture during the PMHS683 tests, it provided detailed information on the belt kinematics during the lap belt to the subject interaction in simulated real world driving conditions. It should be noted that the torso of the PMHS was more reclined (C7 was located about 50 to 65 mm rearward than that of the normal driving posture).

ACKNOWLEDGEMENTS
The author would like to acknowledge and thank the Hyundai Motor Group for funding this research and providing valuable participation, review and feedback throughout the process. The opinions, findings, and conclusions expressed in this manuscript are those of the authors and do not necessarily reflect the views of the Hyundai Motor Group. Additionally, the author would like to acknowledge Rob Salzar, Dennis Roethlisberger and Sara Heltzel for helping the test, Joey White for manufacturing the test rig, and Tim Gillispie for the proofread.

REFERENCES

ADOMEIT, D. & HEGAR, A. 1975. Motion Sequence Criteria and Design Proposals for Restraint Devices in Order to Avoid Unfavorable Biomechanic Conditions and Submarining. *SAE Technical Paper 751146.* SAE International.

FOSTER, C. D., HARDY, W. N., YANG, K. H., KING, A. I. & HASHIMOTO, S. 2006. High-speed seatbelt pretensioner loading of the abdomen. *Stapp car crash journal,* 50**,** 27-51.

LAMIELLE, S., CUNY, S., FORET-BRUNO, J., PETIT, P., VEZIN, P., VERRIEST, J. & GUILLEMOT, H. 2006. Abdominal injury patterns in real frontal crashes: influence of crash conditions, occupant seat and restraint systems. *Annual proceedings / Association for the Advancement of Automotive Medicine. Association for the Advancement of Automotive Medicine,* 50**,** 109-24.

LAMIELLE, S., VEZIN, P., VERRIEST, J.-P., PETIT, P., TROSSEILLE, X. & VALLANCIEN, G. 2008. 3D deformation and dynamics of the human cadaver abdomen under seatbelt loading. *Stapp car crash journal,* 52**,** 267-94.

LUET, C., TROSSEILLE, X., DRAZETIC, P., POTIER, P. & VALLANCIEN, G. 2012. Kinematics and dynamics of the pelvis in the process of submarining using PMHS sled tests. *Stapp car crash journal,* 56**,** 411-42.

POPLIN, G. S., MCMURRY, T. L., FORMAN, J. L., HARTKA, T., PARK, G., SHAW, G., SHIN, J., KIM, H. J. & CRANDALL, J. 2015. Nature and etiology of hollow-organ abdominal injuries in frontal crahses. *Accident Analysis & Prevention,* (in press).

REED, M. P., EBERT, S. M. & HALLMAN, J. J. 2013. Effects of driver characteristics on seat belt fit. *Stapp car crash journal,* 57**,** 43-57.

SALZAR, R., LAU, S., LESSLEY, D., SOCHOR, M., SHAW, C., KENT, R. & CRANDALL, J. 2013. Thoracic response to shoulder belt loading: comparison of tabletop and frontal sled tests with PMHS. *Traffic Inj Prev. ,* 14**,** 159-67.

URIOT, J., BAUDRIT, P., POTIER, P., TROSSEILLE, X., PETIT, P., GUILLEMOT, H., GUERIN, L. & VALLANCIEN, G. 2006. Investigations on the belt-to-pelvis interaction in case of submarining. *Stapp car crash journal,* 50**,** 53-73.